Published in final edited form as:

Clin Cancer Res. 2019 September 01; 25(17): 5329–5341. doi:10.1158/1078-0432.CCR-18-3784.

Modulation of Target Antigen Density Improves CAR T Cell Functionality and Persistence

Sneha Ramakrishna[1], **Steven L Highfill**[2], **Zachary Walsh**[1,3,4], **Sang M Nguyen**[1], **Haiyan Lei**[1], **Jack F. Shern**[1], **Haiying Qin**[1], **Ira Kraft**[1], **Maryalice Stetler-Stevenson**[5], **Constance M. Yuan**[5], **Jennifer Hwang**[6], **Yang Feng**[6], **Zhongyu Zhu**[6], **Dimiter Dimitrov**[6], **Nirali N. Shah**[1], **Terry J. Fry**[1,4]

[1]Pediatric Oncology Branch, National Cancer Institute/ Center for Cancer Research, National Institute of Health, Bethesda, MD

[2]Cell Processing Section, Department of Transfusion Medicine, National Institutes of Health Clinical Center, Bethesda, MD

[3]Colgate University, Hamilton, NY

[4]Department of Pediatrics, University of Colorado Denver and Children's Hospital Colorado, Aurora, CO

[5]Laboratory of Pathology, National Cancer Institute/ Center for Cancer Research, National Institute of Health, Bethesda, MD

[6]Protein Interactions Section, Cancer and Inflammation Program, National Cancer Institute/ Center for Cancer Research, National Institute of Health, Frederick, MD.

Abstract

Purpose: Chimeric antigen receptor T cell (CART) therapy targeting CD22 induces remission in 70% of patients with relapsed/refractory acute lymphoblastic leukemia (ALL). However, the majority of post-CD22 CART remissions are short and associated with reduction in CD22 expression. We evaluate the implications of low antigen density on the activity of CD22 CART and propose mechanisms to overcome antigen escape.

Experimental Design: Using ALL cell lines with variable CD22 expression, we evaluate the cytokine profile, cytotoxicity, and *in vivo* CART functionality in the setting of low CD22 expression. We develop a high-affinity CD22 CAR as an approach to improve CAR sensitivity. We also assess Bryostatin1, a therapeutically relevant agent, to upregulate CD22 and improve CAR functionality.

Corresponding Author: Terry J. Fry, MD, Center for Cancer and Blood Disorders, Children's Hospital, Colorado, University of Colorado Anschutz Medical Campus, 13123 East 16th Ave, Box B115, Aurora, CO 80045, terry.fry@ucdenver.edu, Tel: 720/777.6458, Fax: 720/777.7339.

Current Affiliations: SR – Stanford University, Stanford, CA. DSD – University of Pittsburgh Medical School, Pittsburgh, PA. ZZ - Lentigen Technology Inc., Gaithersburg, MD

Conflicts of Interest: The authors declare no potential conflicts of interest.

Results: We demonstrate that low CD22 expression negatively impacts *in vitro* and *in vivo* CD22 CART functionality and impairs *in vivo* CART persistence. Moreover, low antigen expression on leukemic cells increases naïve phenotype of persisting CART. Increasing CAR affinity does not improve response to low-antigen leukemia. Bryostatin1 upregulates CD22 on leukemia and lymphoma cell lines for 1 week following single-dose exposure, improves CART functionality and *in vivo* persistence. While Bryostatin1 attenuates IFN-gamma production by CART, overall *in vitro* and *in vivo* CART cytotoxicity is not adversely affected. Finally, administration of Bryostain1 with CD22 CAR results in longer duration of *in vivo* response.

Conclusions: We demonstrate that target antigen modulation is a promising strategy to improve CD22 CAR efficacy and remission durability in patients with leukemia and lymphoma.

Keywords

Pediatric Cancers; Immunotherapy/Cellular Immunotherapy; Hematological cancers/leukemias; Chimeric Antigen Receptor

Introduction:

While overall survival for pediatric B-cell acute lymphoblastic leukemia (ALL) treated with risk-adapted, multi-agent chemotherapeutic regimens is greater than 85% at 5 years, patients who relapse lack therapeutic options offering high likelihood of cure(1, 2). For these patients, chimeric antigen receptor T cells (CART) targeting CD19 can induce remissions in a high percentage of patients and is potentially curative (3–5). However, longer follow-up data has now shown that a portion of the patients achieving remission will subsequently relapse with either poor CART persistence or loss of the targeted CD19 epitope (5–8). We developed a CAR targeting CD22 (9), an alternative clinically validated ALL antigen (10), and demonstrated a 70% remission induction rate at biologically active doses, including activity in patients relapsing with CD19 CAR resistant ALL (11). Similar to CD19 CART, remission durability is reduced in a substantial number of patients achieving remission after CD22 CART due to poor CAR persistence or altered target antigen expression (11). However, in contrast to most resistant leukemias relapsing after CD19 CAR or blinatumomab, relapse after the CD22 CAR typically occurs with sustained, but diminished, cell surface CD22 expression on the leukemia (11).

As experience with CAR therapy expands, thresholds of antigen expression required to activate CARs have been identified in preclinical models (12–15). At lower target antigen site densities, CARs are less functional, producing less cytokines such as IFN-gamma or IL-2, despite augmentation with co-stimulatory molecules or alterations of CART binding affinity (13). Importantly, this threshold for activation is relatively high compared to that required for activation through the T cell receptor (16–18). However, the functional ramifications of this site density limitation are not fully understood and the implications of site density on *in vivo* CART cell behavior have not been evaluated. We have extensively studied CD22 site density on a variety of B-cell malignancies, as well as normal B-cells (19). While normal B cell CD22 site density values are approximately 10^4 molecules/cell (19), mean ALL CD22 site density is a log lower, with a wide range in expression, from 10^2 – 10^4 (20). Additionally, specific ALL subtypes such as MLL-rearranged ALL have even

lower CD22 site density (20). These characteristics of CD22 make it a clinically relevant model of reduced antigen expression to evaluate the effects of site density on CART efficacy.

With the goal of developing approaches to overcome immune escape, we systematically evaluated the impact of CD22 site density on CART functionality. Our data demonstrates reduced CART activity, shortened CART persistence, and altered CART phenotype following *in vivo* exposure to leukemia with lower antigen site density. We identified a therapeutically feasible approach to enhance CART efficacy through increasing site density using Bryostatin1, a natural product originally isolated from the marine bryozoan Bugula neritina previously shown to modulate Protein Kinase C (PKC) (21). We found that Bryostatin1, previously shown to up-regulate CD22 expression in chronic lymphocytic leukemia (CLL) (22), increases CD22 expression on pre-B ALL and diffuse large B cell lymphoma (DLBCL), and improves anti-leukemia CART response, memory T cell formation, and durability of response. This is the first report to validate target antigen modulation as a clinically feasible and relevant approach to enhance the efficacy and durability of CART therapy.

Materials and Methods:

Clinical Trial and Patient Data

Patients screened for enrollment on CD19 CART (NCT02028455) or CD22 CART (NCT02315612) trials at the NCI were evaluated for site density of both CD19 and CD22 antigens on the surface of leukemic blasts, measured using flow cytometric methods as previously described, particularly relevant to CD22 detection(REF: PMID: 20872890). Both protocols were approved by the NCI Institutional Review Board and the NIH Recombinant DNA Advisory Committee and were in accordance with U.S. Common Rule. All subjects provided written informed consent, or parental permission with minor assent was obtained when appropriate. Patients treated on the CD22 CAR trial also had serial evaluations for CD22 at the time of enrollment and at relapse. Additionally, four CD22 CART trial patients were evaluated for CAR T cell expansion over time by flow cytometry.

Cell lines, patient-derived xenografts, and healthy donor lymphocytes

B-ALL cell lines used included Nalm6 GFP luciferase transduced, obtained from Dr. Crystal Mackall, 2008, and SEM GFP luciferase transduced and Kopn8 GFP luciferase transduced, obtained from Dr. Sarah Tasian, 2014. Previously generated CRISPR variants of Nalm6-GFP + cell line were used, including $CD22^{neg}$, $CD22^{lo}$, and $CD22^{hi}$ (11). DLBCL cell lines used included Pfeiffer and Toledo, obtained from ATCC in June 2017. All cell lines were routinely tested for *Mycoplasma* by Luminescence Mycoplasma Test (Cambrex MycoAlert), last tested in 2016. All experiments were done within 2 weeks of thawing cell line. Leukemia and lymphoma cell lines, were cultured in RPMI medium supplemented with 10% heat-inactivated FBS, 100 U/mL penicillin, 100 U/mL streptomycin, 2 mM L-glutamine, and 10mM HEPES. Human healthy donor peripheral blood mononuclear cells (PBMCs) were obtained from the Department of Transfusion Medicine at the National Institute of Health under an institutional review board-approved protocol and were frozen in 10% FBS and stored in liquid nitrogen for future use.

The patient-derived xenograft (PDX) in this study was developed from a patient who relapsed with CD22-low leukemia following CD22 CART. The PDX cell line was created by injecting 1×10^6 to 10×10^6 patient ALL cells intravenously into NSG mice (NOD scid gamma, NOD.Cg-*Prkdcscid Il2rgtm1Wjl*/SzJ; Jackson ImmunoResearch Laboratories). After the second passage, the cell line was transduced with a lenti-GFP-Luc virus and sorted for the leukemia cells expressing GFP luciferase.

Generation of site density model

As described previously, site density model cell lines were developed through CRISPR/Cas9 editing to remove CD22, followed by lentiviral reinsertion of CD22 and single cell cloning (11). For additional details, please see supplementary methods.

Generation of human CD22 CAR T cells

Lentiviral vectors encoding CD22 CAR were produced by transient transfection of 293T cells. Using Lipofectamine 3000 (Life Technologies), 293T cells were transfected with plasmids encoding packing and envelope vectors (pMDLg/pRRE, pMD.2G, pRSV-Rev, p3000), as well as a plasmid encoding the CD22-CAR. Viral supernatant was harvested from transfected cells at 24, 48, and 72 hours after transfection, spun for 10 minutes at 3000 RPM to remove cell debris, and frozen at −80C. Human lymphocytes were then thawed at 1×10^6/mL and activated for 48 hours in AIM-V media with 40 IU/mL IL-2 and a 3:1 ratio of CD3/CD28 microbeads (Life Technologies) per cell. T cells were then re-suspended at 2×10^6/mL in 10 mL lentiviral supernatant, 5 mL AIM-V, 100 IU IL-2, and 10 ug/mL protamine sulfate, and subsequently spun at 2000G for 2 hours at 32°C in 6-well plates. Plates were then incubated overnight at 37°C, and the process was repeated for a second day. After the second overnight incubation, CD3/CD28 microbeads were removed, T cells were re-suspended at 0.3×10^6/mL in AIM-V with 100 IU/mL IL-2, and were cultured for an additional 48–72 hours before use in experiments. After generation, T cells (both CAR and mock) were cultured in AIM-V medium supplemented with 5% heat-inactivated FBS, 100 U/mL penicillin, 100 U/mL streptomycin, 2 mM L-glutamine, 10mM HEPES, and 100 IU/mL IL-2.

Nalm6 Xenograft and Patient-derived Xenograft *in vivo* studies

CD22 CAR functionality and anti-leukemic efficacy were evaluated *in vivo* in Nalm6 xenograft or PDX models with NOD.Cg-Prkdcscid Il2rgtm1Wjl/SzJ (NSG) mice (The Jackson Laboratory and bred in house) aged 6–10 weeks. Mice received 1×10^6 GFP+ Luciferase+ tumor cells (Nalm6, Nalm6 CRISPR variant, or PDX) intravenously on day 0. On day 3, mice received CD22-CAR-transduced T cells or mock-transduced T cells intravenously at the indicated quantity. To monitor leukemia burden, luciferin-D (Caliper Life Sciences) was injected into mice intraperitoneally and imaged 4 minutes later using In Vivo Imaging System (IVIS) technology (Caliper Life Sciences). Bioluminescent signal flux (luminescence) for mice was measured using Living Image Version 4.1 software (Caliper Life Science). All animal studies were conducted in accordance with an approved animal protocol (PB-027–2-M) with the National Cancer Institute Animal Care and Use Committee.

Bryostatin1 treatment

For all *in vitro* experiments and tumor/CAR pretreatment prior to intravenous injection, Bryostatin1 was administered to cells at a concentration of 1 ng/mL (1nM). Dimethyl sulfoxide (DMSO) vehicle control was administered to control-treated cells at an equal volume. Prior to co-culture or intravenous injection, Bryostatin1- and DMSO- treated cells were washed three times in sterile PBS. For all *in vivo* experiments, Bryostatin1 was diluted in PBS and administered via intraperitoneal injection at 40 ug/kg (1ug/25g mouse). For control-treated groups, an equal volume of DMSO was diluted in PBS and administered in the same manner.

RNA Sequencing and data analysis

16 RNA-seq samples were pooled and sequenced on one NextSeq high output run using Illumina TruSeq Poly A RNA Kit v3 with paired end sequencing. All samples had greater than 30 million reads pass filter reads with a base call quality of above 95% of bases with Q30 and above. Reads of the samples were trimmed for adapters and low-quality bases using Trimmomatic software before alignment with the reference genome Human - hg19 and the annotated transcripts using STAR. The mapping quality statistics were calculated using Picard software and library complexity was measured in terms of unique fragments in the mapped reads using Picard's MarkDuplicate utility. The Partek Flow informatics pipeline was used to generate fold change and differentially expressed gene data as well as for data visualization. GSEA analysis of the differentially expressed genes was performed as previously described and using standard parameters.

Flow cytometry

FACS analysis of cell surface CAR and protein expression was performed using an LSR II Fortessa flow cytometer (BD Biosciences). CD22-CAR was detected by incubation with 22-Fc (R&D Systems), followed by incubation with human IgG-specific PE-F(ab)2 (Thermo Fisher Scientific). The following human monoclonal antibodies were used for detection of cell surface proteins: CD22-APC, CD22-PE, CD19-Pacific Blue, CD45-PerCP/Cy5.5, CD3-APC/Cy7, PD1-PE/Cy7, LAG3-APC, TIM3-Pacific Blue, CD8-APC, CD8-PE/Cy7, CD45RA-APC, CD45RO-PE/Cy7, CCR7-Pacific Blue, CD4-Pacific Blue, CD69-APC (all from BioLegend). CD22 site density was determined using QuantiBrite-PE beads (BD Biosciences) using methods previously described (PMID: 20872890). Dead cells were identified using eFluor 506 fixable viability dye (Thermo Fisher Scientific). GFP-expressing leukemia was identified through the FITC channel.

In vitro cytokine and leukemia clearance assays

Cytokine production assays: CAR or mock T cells were washed to remove IL-2 and re-suspended in RPMI medium. 1×10^5 effector cells were then co-cultured with tumor cells in RPMI at a 1:1 effector to target ratio in 96-well plates and incubated at 37°C for 20 hours. Plates were spun at 1200 RPM for 6 minutes to pellet the cells, and cytokine concentrations in the culture supernatants were measured using IL-2 ELISA (R&D systems), IFN-gamma ELISA (R&D systems), or Granzyme B ELISA (Thermo Fisher Scientific) kits according to the manufacturer's directions.

Leukemia clearance assays: 1×10^5 CAR or mock T cells were co-cultured with tumor cells in RPMI at a 1:1 effector to target ratio in 96-well plates. After initiation of co-culture, plates were incubated in an IncuCyte ZOOM and imaged for green object confluence (indicating GFP positive leukemia confluence) every 3–6 hours for up to 40 hours.

Statistics

ELISA and *in vitro* flow cytometry results were compared by student's unpaired t-test. CAR protein expression changes in bone marrow, spleen, and peripheral blood were calculated using the Mann-Whitney test.

Results:

Decreased CD22 site density on Pre-B cell ALL impacts CD22-directed CART functionality.

CD22 site density on ALL leukemic blasts is significantly lower than CD19 site density (23). We have previously shown that leukemic blasts from patients with refractory ALL treated with CD22 CART therapy demonstrated a significant decline in CD22 site density at relapse compared to pre-treatment (11), and we now validate these findings that 8/20 CD22 CAR-treated patients relapsed with a 50% reduction of CD22 expression (Fig. 1A; median site density pre-CAR 2714, post-CAR median 1435). Patients with lower initial blast CD22 site density tended to have decreased CD22 CAR expansion (Fig. 1B). Moreover, the patients with lower initial CD22 site densities were only able to maintain stabilization of disease (SD), while patients with higher initial site density achieved an MRD-negative complete response (CR) (Fig. 1B). Collectively, these observations suggest that the lower and dynamic expression of CD22, as compared to CD19, impacts CART activity.

To determine whether CD22 site density directly impacts CART function, we generated Nalm6 ALL cell lines with varying expression of CD22, and selected four specific cell lines to represent a range of clinically relevant antigen expressions (CD22-negative ($CD22^{neg}$), CD22-low ($CD22^{lo}$, 621 molecules/cell), parental Nalm6 (Nalm6, 1998 molecules/cell), and CD22-high ($CD22^{hi}$, 12007 molecules/cell)) (Supplementary Fig. S1A) (11). In co-culture assays, healthy, donor-derived CD22 CART produced incrementally decreased IFN-gamma, IL-2, and Granzyme B in response to lower CD22 antigen site densities (Supplementary Fig. S1B) (11). To account for donor variability affecting CART functionality, we assessed the CD22 CAR products from 17 patients enrolled on our CD22 CART trial, which confirmed the gradation of IL-2 production relative to site density (Fig. 1D). There was a consistent pattern of diminished production of multiple T cell cytokines by patient-derived CD22 CART products in response to low CD22-expressing cell lines (Supplementary Fig. S1C).

Site density affects CD22 CART activation, efficacy, expansion and phenotype.

While low CD22 site expression did not affect CART-mediated eradication of ALL *in vitro, in vivo* clearance of $CD22^{lo}$ ALL by CD22 CART was impaired compared to clearance of parental Nalm6, as previously shown (11). Moreover, eradication of $CD22^{lo}$ ALL was not rescued by increased dose of CD22 CART (Fig. 1D). Importantly, diminished ability for CD22 CART to clear $CD22^{lo}$ ALL was associated with poor early expansion of CART (Fig. 1E), consistent with our observations in patients treated with the CD22 CART (Fig. 1B).

Finally, CD22 CART were significantly reduced in the bone marrow of $CD22^{lo}$ leukemia-bearing mice at day 16 after CAR injection as compared to parental Nalm6-bearing mice (Fig. 1F). Together, these findings demonstrate that CD22 CART are less effective at clearing $CD22^{lo}$ ALL due to ineffective CAR expansion.

We next assessed the impact of site density on the activation of CART during initial expansion. PD-1 expression on CART was reduced by 30% after 24 hours of *in vitro* co-culture with $CD22^{lo}$ ALL compared to parental Nalm6 (Figure 2A). Following 8 days of *in vitro* co-culture, $CD22^{lo}$-exposed CARs had a higher percentage of naïve cells (CCR7+, CD45RA+) compared to Nalm6-exposed CARs (Fig. 2B). When evaluated *in vivo*, there was no difference in CAR PD1 expression at day 16, and by day 30 there was only a modest decrease in PD1 expression on persisting CD22 CART in the $CD22^{lo}$ leukemia group as compared to the Nalm6-bearing group (Fig. 2C). *In vivo* analysis of CART phenotype 16 days after injection showed a marked change in the CCR7 and CD45RA profile and a trend toward more naïve cells following $CD22^{lo}$ leukemia exposure compared to Nalm6 exposure (Fig. 2D). This combined *in vitro* and *in vivo* data suggests that, in the presence of low antigen density, CART may not be able to convert to a memory phenotype, thereby resulting in decreased durability of response *in vivo*.

Increased CAR affinity does not improve CAR sensitivity to low site density leukemia.

The CD22-specific scFv (m971) used in the construction of the CD22 CAR has a relatively low binding affinity (9, 24). Thus, we modified the anti-CD22 scFv (m971-L7) to generate a higher affinity CD22 CAR ($CD22^{V1}$ CAR) (Supplementary Fig. S2A) with improved binding at lower antigen densities, while maintaining the same 41BB costimulatory domain. However, this scFv modification did not enhance *in vitro* cytokine production or cytotoxicity (Fig. 3A–B). Furthermore, the $CD22^{V1}$ CAR did not improve clearance of $CD22^{lo}$ leukemia cells in xenografts (Fig. 3C). To evaluate the cause of this lack of enhanced activity *in vitro*, T cells expressing the $CD22^{V1}$ CAR were evaluated for persistence, activation, exhaustion, and memory phenotype both *in vitro* and *in vivo*. One day after co-culture with $CD22^{lo}$ leukemia, the $CD22^{V1}$ CAR had similar PD1 expression as the original CAR (Supplementary Fig. S2B). However, both on Day 1 and Day 8 of *in vitro* co-culture, a higher percentage of $CD22^{V1}$ CART remained naïve compared to the original CD22 CAR (Fig. 3D). $CD22^{V1}$ CART persisted in the presence of $CD22^{lo}$ leukemia *in vivo* at Day 16 (Fig. 3E), with similar expression of PD1, TIM3 and LAG3 compared to the original CAR (Supplementary Fig. S2C). Similar to the *in vitro* findings, a higher percentage of $CD22^{V1}$ CART remained naïve as compared to the original CD22 CAR when responding to both $CD22^{lo}$ and parental Nalm6 leukemia (Fig. 3F and Supplementary Fig. 2E). Finally, a population of EMRA CART (CCR7-, CD45RA+), consistent with terminal differentiation, emerged in the $CD22^{V1}$ CAR, that was not present in the original CD22 CAR and that was more pronounced when targeting $CD22^{lo}$ leukemia (Fig. 3F and Supplementary Fig. S2F).

Bryostatin1 increases CD22 antigen expression on ALL and DLBCL cell lines.

We hypothesized that CART activity could be improved through a drug-mediated increase in antigen expression. Bryostatin1 has been shown to increase CD22 on CLL (22). Thus, we tested the impact of Bryostatin1 on CD22 expression in two pre-B ALL cell lines and two

diffuse large B cell lymphoma (DLBCL) cell lines. All four cell lines demonstrated an increase in CD22 expression upon exposure to Bryostatin1 at 1nM *in vitro* (Fig. 4A). Bryostatin1 did not alter CD19 expression on ALL cell lines, but a modest increase was observed on DLBCL cell lines (Fig. 4A). Interestingly, increased CD22 expression persisted and, in fact, increased at one week following removal of Bryostatin1 (Fig. 4B). Furthermore, a single dose of Bryostatin1 administered intraperitoneally (I.P.) increased CD22 MFI on Nalm6 for 1 week, followed by a return to baseline expression 12 days post-drug administration (Fig. 4C). Finally, we confirmed that Bryostatin1 upregulated CD22 on a CD22-low relapse patient-derived ALL xenograft (Fig. 4D).

Bryostatin1-mediated CD22 upregulation may occur via mechanisms other than increased CD22 gene expression mediated by PKC inhibition.

Consistent with previous reports in CLL (22), PKCβII protein levels decreased in ALL cells upon exposure to Bryostatin1 (Supplementary Fig. S3A), suggesting a similar PKC-driven mechanism of CD22 upregulation. However, neither the PKCβII inhibitor, Enzastaurin, nor a broad PKC inhibitor, Staurosporine, were able to upregulate CD22 (Supplementary Fig. S3B). To further interrogate potential mechanisms of CD22 upregulation, we performed RNA-sequence analysis (RNAseq) on two Bryostatin1-treated and -untreated MLL-rearranged ALL cell lines [KOPN8 (MLL-MLLT1 fusion oncogene) and SEM (MLL-AFF1 fusion oncogene)] – both of which show robust upregulation of CD22 with Bryostatin1 exposure (Supplementary Fig. S4A). There were marked differences between the two cell lines in the magnitude of the transcriptional response to Bryostatin1 (Fig. 5A). While both of these cell lines represent MLL-rearranged tumors, KOPN8 demonstrated 1524 genes with a greater than 2-fold change at 24 hours, whereas only one gene demonstrated a 2-fold change with Bryostain1 exposure in SEM, indicating variability in leukemic response to Bryostatin1. Nonetheless, by lowering the threshold to a fold change of 1.5, a common set of genes could be found to be altered in both SEM and KOPN8, including several cell surface proteins such as CD82, FLT1, FGFR1, and TLR10 (Supplementary Fig. S4B), suggesting potential specificity of Bryostatin1 to cell surface molecules. Interestingly, neither cell line demonstrated changes in the CD22 mRNA over the course of Bryostatin1 treatment (Fig. 5B). Using the 756 genes with 2-fold increased expression versus control in KOPN8 and gene set enrichment analysis (GSEA) we found significant enrichment in genes known as intrinsic components of the plasma membrane (Supplementary Table S1). Finally, Bryostatin1-treated cells contained less vacuolized CD22 at 24 hours after exposure compared to DMSO controls suggesting that the increase in CD22 surface expression mediated by Bryostatin1 may involve changes in membrane trafficking (Supplementary Fig. S4C).

In vitro CD22 CART functionality, but not CD19 CART, is enhanced following Bryostatin1 priming of leukemia cells.

We next sought to determine whether Bryostatin1-mediated increase in CD22 site density on leukemic cells could enhance the functionality of CD22 CART. Bryostatin1 pre-treatment of both B-ALL and DLBCL cell lines significantly enhanced *in vitro* production of IL-2, IFN-γ and Granzyme B by the CD22 CAR (Fig. 5C–E). Conversely, the CD19 CAR did not show improved Granzyme B production with the leukemia-exposure to Bryostatin1

(Supplementary Fig. S5A). However, Bryostatin1 did not reduce efficacy of the CD19 CAR *in vivo* (Supplementary Fig. S5B).

Exposure of CART to Bryostatin1 attenuates cytokine production but does not affect *in vitro* or *in vivo* cytotoxicity.

Bryostatin1 modulates PKC isoforms which play an important role in T cell receptor signaling pathways (25, 26). With the ultimate goal of utilizing Bryostatin1 in combination with CAR therapy, we evaluated the direct impact of Bryostatin1 on CD22 CAR functionality, independent of its effects on leukemic site density. CD22 CAR pre-treated with Bryostatin1 produced attenuated levels of IFN-γ when subsequently co-cultured with ALL or DLBCL cell lines relative to DMSO-control pre-treated CD22 CAR, but produced significantly increased levels of Granzyme B (Fig. 5F–G). *In vitro* cytotoxicity kinetics of Bryostain1-exposed CART were similar to DMSO-exposed CART (Fig. 5H). To evaluate the combined effect of Bryostatin1 on leukemic CD22 site density and CART functionality we repeated functional assays using Bryostatin1-treated leukemia with Bryostatin1-exposed CART. Attenuated IFN-γ production by CART-exposed cells was restored (Fig. 5F) and Granzyme B production was augmented (Fig. 5G) in the presence of Bryostatin1 pre-treated leukemia cells. Finally, we evaluated Bryostatin1 effects on *in vivo* CAR activity against $CD22^{lo}$ leukemia, which does not modulate CD22 expression following Bryostatin1 exposure (Supplementary Fig. S4D). Bryostatin1 did not impact the ability of the CD22 CAR to attenuate progression of the $CD22^{lo}$ leukemia or CD22 CAR ability to clear the Nalm6 leukemia *in vivo* (Fig. 5I and Supplementary Fig. S6A). Together, these findings demonstrate that exposing CART to Bryostatin1 affects IFN-gamma and Granzyme B production, but does not negatively impact overall CART functionality *in vivo*.

Bryostatin1 affects CART persistence, memory phenotype, and improves durability of leukemic response.

Finally, we evaluated the impact of Bryostatin1-mediated increase in CD22 site density on *in vivo* CAR persistence and functionality using the parental Nalm6 which does not express sufficient CD22 to maximize cytokine response (Supplementary Fig.S1) and does modulate CD22 expression in response to Bryostatin1 (Fig. 4). We tested the administration of Bryostatin1 as a “priming therapy” prior to CART infusion. Mice were injected with Bryostatin1 pre-treated tumor cells, followed by CART injection. Seven days after CD22 CAR injection, T cell phenotype was evaluated. Within the CD8+ CART population, we found significant cumulative enrichment of central memory (CCR7+, CD45RA-) and effector memory (CCR7-, CD45RA-) cells, and fewer naive cells, in the spleens of mice that received Bryostatin1 pre-treated Nalm6 (Fig. 6A). With Bryostatin1 exposure, CART demonstrated similar activation without evidence of exhaustion, as evidenced by stable PD1 expression, without increase in TIM3 or LAG3 (Supplementary figure Fig. S5A). At 30 days, mice treated with Bryostatin1 after CART injection had slightly increased CD22 CART in bone marrow (Fig. 6B). We then tested Bryostatin1 administration for two weeks after sub-curative dose of CD22 CART infusion in Nalm6 (Fig. 6C and Supplementary Fig. 6B) and SEM (Fig. 6C and Supplementary Fig. S6C), demonstrating that Bryostatin1 improved durability of remission, extending beyond cessation of Bryostatin1. Finally, we evaluated the effects of Bryostatin1 administration following CD22 CART infusion the

CD22-low relapse PDX model, demonstrating improved ability to clear leukemia (Fig. 6D and Supplementary Fig. 6D). Collectively, these results demonstrate that Bryostatin1 is effective as both a priming therapy to increase antigen expression prior to CAR T cell infusion and as a potential rescue following emergence of CD22 CAR resistant leukemia.

Discussion:

CAR T cell therapy has provided patients with relapsed or refractory pre-B cell ALL a potentially curative therapeutic option, but remission duration is shortened in a high percentage of patients due to changes in target antigen expression. Furthermore, recent studies have begun to identify limitations in CAR activity in the setting of low antigen site density (11–15, 27–33). Our recent clinical experience with a CD22 CAR supports low antigen density as a mechanism of escape from CAR-targeted therapy (11). Here, we evaluate the characteristics of CAR failure in the setting of low site density, focusing on the effects on CAR function and persistence. Moreover, we provide the first preclinical evidence to support the use of drug-mediated antigen modulation to overcome such limitations. Our data establishes two important findings: (A) low site density on tumor cells results in significant changes in the persistence and phenotype of CART, and (B) drug-mediated increase in target antigen site density improves CAR T cell functionality and length of remission.

We first assessed the effects of site density on short-term CART functionality, and observed a reduction in cytokine production as target antigen expression declines, consistent with previous studies (12, 15, 32, 33). We further demonstrate that the CD22 CAR delayed *in vivo* progression of, but failed to clear, low site density leukemia. Although activation and exhaustion markers, including PD1, TIM3, and LAG3, were not significantly different on CART exposed to low site density leukemia, lower site density leukemia induced a significant decrease in numbers of persisting CART, with a more naïve memory phenotype, suggesting diminished T cell expansion and conversion to memory phenotype. Whether this finding represents a recruitment of less CAR-expressing T cells into the expansion pool or less potent activation of the same percentage of CAR expressing T cells will require further testing. This is the first clear evidence that site density not only affects short-term activity of CART, but also affects long-term persistence, with implications for the durability of CART-induced remissions. However, as these findings were in a xenograft model, it is impossible to ascertain the exact implications for CAR persistence in an immune competent host, in which non-leukemic expression of CAR antigen could impact sustained expansion of the CART. Thus, these findings require confirmation in immune competent models or in patients.

We next proceeded to evaluate potential strategies to overcome the limitations on cellular therapy imposed by low antigen density, through either improving CAR functionality or augmenting tumor sensitivity. We attempted to improve CAR functionality through enhancing the affinity of the CD22 CAR, thereby improving sensitivity to low site density. Although binding affinity can improve the efficacy of soluble antibody-based therapeutics (34), our data does not demonstrate improvement in CAR functionality with increased scFv affinity. Interestingly, while $CD22^{V1}$ CAR had a larger naïve T cell population, especially

against $CD22^{lo}$ leukemia, it also demonstrated a more pronounced terminally differentiated effector memory population (CCR7-, CD45RA+), suggesting that when the T cell is activated by the $CD22^{V1}$ CAR, it may become terminally differentiated rather than converting to a memory phenotype. While this data is supported by experience with some CARs (35), the complexity of individual CAR constructs may preclude the ability to generalize these findings (28, 36).

To improve tumor sensitivity, we found that Bryostatin1 upregulated CD22 expression in ALL and DLBCL cell lines, as well as in a CD22-low relapse patient-derived xenograft, thereby improving CART cytokine production and memory phenotype. As a modulator of PKC, Bryostatin1 has variable effects on PKC protein levels based on exposure parameters (37–41). In CLL cell lines, Bryostatin1-mediated upregulation of CD22 correlated with decreased PKC (22). We found that Bryostatin1 was associated with decreased PKC-ßII, but PKC inhibitors did not provide the same upregulation of CD22 as Bryostatin1. We also found that CD22 mRNA levels were not significantly altered in Bryostatin1-treated ALL cell lines and that multiple cell surface molecules were upregulated. These findings suggest that Bryostatin1 has a much more complex mechanism of upregulation of CD22, but further evaluation will be needed to elucidate the exact mechanism of CD22 upregulation.

We demonstrate that CAR functionality can be indirectly improved via Bryostatin1-mediated increase in CD22 expression. However, Bryostatin1 has been previously implicated in directly affecting T cell function (25, 26). Although Bryostatin1 attenuated IFN-gamma production by CD22 CART, Granzyme B production was increased and there was ultimately no adverse effect on *in vitro* or *in vivo* cytotoxicity. The net effect of Bryostatin1 on CART functionality and antigen expression level resulted in overall augmented cytokine production and cytotoxicity, and improved durability of response. This indicates that Bryostatin1 could be administered during CART expansion or to rescue patients following post-CART relapse resulting from reduced antigen expression. However, we also postulate that Bryostatin1 could be used to prime tumors prior to CART therapy based on our observation that site density affects CAR T cell persistence.

While combination therapies are the cornerstone of oncologic treatments, CART have not yet been combined with other drugs with the intent of augmenting sensitivity to low antigen levels. Prior pre-clinical studies have shown improved CAR activity with drug modulation (14, 42); however, to our knowledge, our findings are the first to describe how drug-induced increased antigen expression can improve CAR T cell activity. Bryostatin1 has been used in clinical trials for oncologic patients with more than 1,400 individuals treated, including one phase I pediatric clinical trial. The pediatric phase I study showed the drug to be well-tolerated, but recommended increasing the dose administration in subsequent trials (43). While adult phase I and II studies have established the maximum tolerated dose, the measured effect was tumor response and PKC inhibition rather than surface protein expression. Our data supports the concept of using Bryostatin1 to modulate target antigen density in combination with a targeted immunotherapy such as CART, but clinical experience is needed in pediatric patients specifically characterizing CD22 antigen expression as a biomarker to establish Bryostatin1 dosing.

Taken together, our observations contribute to an understanding of the complexity in developing effective CAR therapies in tumors where lower expression is a characteristic of the targeted antigen. Since CD22 expression has been targeted successfully by immunotherapy and is likely comparable to many other antigens currently being evaluated (12, 28), CD22 represents a broadly applicable and clinically relevant model antigen. As such, the effects of antigen expression on CAR persistence and phenotype described here may be pertinent to many other potential target antigens. Finally, our findings with Bryostatin1 support the initiation of trials testing whether drug-mediated upregulation of antigen expression can improve efficacy and remission durability following targeted immunotherapy.

Supplementary Material

Refer to Web version on PubMed Central for supplementary material.

Acknowledgements

We would like to thank John Buckley for his assistance with murine experiments and Dr. Michael Kruhlak for his aid in confocal microscopy. We would also like to thank Drs. Crystal Mackall, Patrick Brown, Rimas Orentas, and Elena Sotillo for their feedback and comments. This work was supported by the Intramural Research Program at the NIH and by a St. Baldrick's Foundation - Stand Up To Cancer Pediatric Cancer Dream Team Translational Research Grant (Grant Number: SU2C-AACR-DT-27–17). Stand Up To Cancer is a division of the Entertainment Industry Foundation. Research grants are administered by the American Association for Cancer Research, the Scientific Partner of SU2C.

Financial Support: This work was supported by the Intramural Research Program at N.I.H. Research reported in this publication was supported in part by funds provided by UPMC (University of Pittsburgh Medical Center) as part of the UPMC Immune Transplant and Therapy Center. The content is solely the responsibility of the authors and does not necessarily represent the official views of UPMC.

References

1. Pui CH, Yang JJ, Hunger SP, Pieters R, Schrappe M, Biondi A, et al. Childhood Acute Lymphoblastic Leukemia: Progress Through Collaboration. J Clin Oncol. 2015;33(27):2938–48. [PubMed: 26304874]
2. Smith MA, Altekruse SF, Adamson PC, Reaman GH, and Seibel NL. Declining childhood and adolescent cancer mortality. Cancer. 2014;120(16):2497–506. [PubMed: 24853691]
3. Davila ML, Riviere I, Wang X, Bartido S, Park J, Curran K, et al. Efficacy and toxicity management of 19–28z CAR T cell therapy in B cell acute lymphoblastic leukemia. Sci Transl Med. 2014;6(224):224ra25.
4. Maude SL, Frey N, Shaw PA, Aplenc R, Barrett DM, Bunin NJ, et al. Chimeric antigen receptor T cells for sustained remissions in leukemia. N Engl J Med. 2014;371(16):1507–17. [PubMed: 25317870]
5. Lee DW, Kochenderfer JN, Stetler-Stevenson M, Cui YK, Delbrook C, Feldman SA, et al. T cells expressing CD19 chimeric antigen receptors for acute lymphoblastic leukaemia in children and young adults: a phase 1 dose-escalation trial. Lancet. 2015;385(9967):517–28. [PubMed: 25319501]
6. Grupp SA, Kalos M, Barrett D, Aplenc R, Porter DL, Rheingold SR, et al. Chimeric antigen receptor-modified T cells for acute lymphoid leukemia. N Engl J Med. 2013;368(16):1509–18. [PubMed: 23527958]
7. Maude SL, Teachey DT, Porter DL, and Grupp SA. CD19-targeted chimeric antigen receptor T-cell therapy for acute lymphoblastic leukemia. Blood. 2015;125(26):4017–23. [PubMed: 25999455]
8. Gardner R, Wu D, Cherian S, Fang M, Hanafi LA, Finney O, et al. Acquisition of a CD19-negative myeloid phenotype allows immune escape of MLL-rearranged B-ALL from CD19 CAR-T-cell therapy. Blood. 2016;127(20):2406–10. [PubMed: 26907630]

9. Haso W, Lee DW, Shah NN, Stetler-Stevenson M, Yuan CM, Pastan IH, et al. Anti-CD22-chimeric antigen receptors targeting B-cell precursor acute lymphoblastic leukemia. Blood. 2013;121(7):1165–74. [PubMed: 23243285]
10. Yilmaz M, Richard S, and Jabbour E. The clinical potential of inotuzumab ozogamicin in relapsed and refractory acute lymphocytic leukemia. Ther Adv Hematol. 2015;6(5):253–61. [PubMed: 26425338]
11. Fry TJ, Shah NN, Orentas RJ, Stetler-Stevenson M, Yuan CM, Ramakrishna S, et al. CD22-targeted CAR T cells induce remission in B-ALL that is naive or resistant to CD19-targeted CAR immunotherapy. Nat Med. 2017.
12. Walker AJ, Majzner RG, Zhang L, Wanhainen K, Long AH, Nguyen SM, et al. Tumor Antigen and Receptor Densities Regulate Efficacy of a Chimeric Antigen Receptor Targeting Anaplastic Lymphoma Kinase. Mol Ther. 2017;25(9):2189–201. [PubMed: 28676342]
13. Chmielewski M, Hombach AA, and Abken H. CD28 cosignalling does not affect the activation threshold in a chimeric antigen receptor-redirected T-cell attack. Gene Ther. 2011;18(1):62–72. [PubMed: 20944680]
14. Yoshida T, Mihara K, Takei Y, Yanagihara K, Kubo T, Bhattacharyya J, et al. All-trans retinoic acid enhances cytotoxic effect of T cells with an anti-CD38 chimeric antigen receptor in acute myeloid leukemia. Clin Transl Immunology. 2016;5(12):e116. [PubMed: 28090317]
15. Watanabe K, Terakura S, Martens AC, van Meerten T, Uchiyama S, Imai M, et al. Target antigen density governs the efficacy of anti-CD20-CD28-CD3 zeta chimeric antigen receptor-modified effector CD8+ T cells. J Immunol. 2015;194(3):911–20. [PubMed: 25520398]
16. Huang J, Brameshuber M, Zeng X, Xie J, Li QJ, Chien YH, et al. A single peptide-major histocompatibility complex ligand triggers digital cytokine secretion in CD4(+) T cells. Immunity. 2013;39(5):846–57. [PubMed: 24120362]
17. Sykulev Y, Joo M, Vturina I, Tsomides TJ, and Eisen HN. Evidence that a single peptide-MHC complex on a target cell can elicit a cytolytic T cell response. Immunity. 1996;4(6):565–71. [PubMed: 8673703]
18. Srivastava S, and Riddell SR. Engineering CAR-T cells: Design concepts. Trends Immunol. 2015;36(8):494–502. [PubMed: 26169254]
19. Jasper GA, Arun I, Venzon D, Kreitman RJ, Wayne AS, Yuan CM, et al. Variables affecting the quantitation of CD22 in neoplastic B cells. Cytometry B Clin Cytom. 2011;80(2):83–90. [PubMed: 20872890]
20. Shah NN, Stevenson MS, Yuan CM, Richards K, Delbrook C, Kreitman RJ, et al. Characterization of CD22 expression in acute lymphoblastic leukemia. Pediatr Blood Cancer. 2015;62(6):964–9. [PubMed: 25728039]
21. George R. Pettit CLH, Dennis L. Doubek, Delbert L. Herald, Edward Arnold, Jon Clardy. Isolation and structure of bryostatin 1. J Am Chem Soc. 1982;104(24):6846–8.
22. Viola Biberacher TD, Madlen Oelsner, Michaela Wagner, Christian Bogner, Burkhard Schmidt, Robert J. Kreitman, Christian Peschel, Ira Pastan, Christian Meyer zum Büschenfelde, and Ingo Ringshausen. The cytotoxicity of anti-CD22 immunotoxin is enhanced by bryostatin 1 in B-cell lymphomas through CD22 upregulation and PKC-βII depletion. Haematologica. 2012;97(5):771–9. [PubMed: 22180432]
23. Qin H, Ramakrishna S, Nguyen S, Fountaine TJ, Ponduri A, Stetler-Stevenson M, et al. Preclinical Development of Bivalent Chimeric Antigen Receptors Targeting Both CD19 and CD22. Mol Ther Oncolytics. 2018;11:127–37. [PubMed: 30581986]
24. Xiao X, Ho M, Zhu Z, Pastan I, and Dimitrov DS. Identification and characterization of fully human anti-CD22 monoclonal antibodies. MAbs. 2009;1(3):297–303. [PubMed: 20065646]
25. Tuttle TM, Bethke KP, Inge TH, McCrady CW, Pettit GR, and Bear HD. Bryostatin 1-activated T cells can traffic and mediate tumor regression. J Surg Res. 1992;52(6):543–8. [PubMed: 1528028]
26. Drexler HG, Gignac SM, Jones RA, Scott CS, Pettit GR, and Hoffbrand AV. Bryostatin 1 induces differentiation of B-chronic lymphocytic leukemia cells. Blood. 1989;74(5):1747–57. [PubMed: 2506950]

27. Weijtens ME, Hart EH, and Bolhuis RL. Functional balance between T cell chimeric receptor density and tumor associated antigen density: CTL mediated cytolysis and lymphokine production. Gene Ther. 2000;7(1):35–42. [PubMed: 10680014]
28. Turatti F, Figini M, Balladore E, Alberti P, Casalini P, Marks JD, et al. Redirected activity of human antitumor chimeric immune receptors is governed by antigen and receptor expression levels and affinity of interaction. J Immunother. 2007;30(7):684–93. [PubMed: 17893561]
29. James SE, Greenberg PD, Jensen MC, Lin Y, Wang J, Till BG, et al. Antigen sensitivity of CD22-specific chimeric TCR is modulated by target epitope distance from the cell membrane. J Immunol. 2008;180(10):7028–38. [PubMed: 18453625]
30. Anurathapan U, Chan RC, Hindi HF, Mucharla R, Bajgain P, Hayes BC, et al. Kinetics of tumor destruction by chimeric antigen receptor-modified T cells. Mol Ther. 2014;22(3):623–33. [PubMed: 24213558]
31. Caruso HG, Hurton LV, Najjar A, Rushworth D, Ang S, Olivares S, et al. Tuning Sensitivity of CAR to EGFR Density Limits Recognition of Normal Tissue While Maintaining Potent Antitumor Activity. Cancer Res. 2015;75(17):3505–18. [PubMed: 26330164]
32. Hombach AA, Gorgens A, Chmielewski M, Murke F, Kimpel J, Giebel B, et al. Superior Therapeutic Index in Lymphoma Therapy: CD30(+) CD34(+) Hematopoietic Stem Cells Resist a Chimeric Antigen Receptor T-cell Attack. Mol Ther. 2016;24(8):1423–34. [PubMed: 27112062]
33. Hegde M, Mukherjee M, Grada Z, Pignata A, Landi D, Navai SA, et al. Tandem CAR T cells targeting HER2 and IL13Ralpha2 mitigate tumor antigen escape. J Clin Invest. 2016;126(8):3036–52. [PubMed: 27427982]
34. Adler MJ, and Dimitrov DS. Therapeutic antibodies against cancer. Hematol Oncol Clin North Am. 2012;26(3):447–81, vii. [PubMed: 22520975]
35. Arcangeli S, Rotiroti MC, Bardelli M, Simonelli L, Magnani CF, Biondi A, et al. Balance of Anti-CD123 Chimeric Antigen Receptor Binding Affinity and Density for the Targeting of Acute Myeloid Leukemia. Mol Ther. 2017;25(8):1933–45. [PubMed: 28479045]
36. Lynn RC, Feng Y, Schutsky K, Poussin M, Kalota A, Dimitrov DS, et al. High-affinity FRbeta-specific CAR T cells eradicate AML and normal myeloid lineage without HSC toxicity. Leukemia. 2016;30(6):1355–64. [PubMed: 26898190]
37. Isakov N, Galron D, Mustelin T, Pettit GR, and Altman A. Inhibition of phorbol ester-induced T cell proliferation by bryostatin is associated with rapid degradation of protein kinase C. J Immunol. 1993;150(4):1195–204. [PubMed: 8432975]
38. Lee HW, Smith L, Pettit GR, and Bingham Smith J. Dephosphorylation of activated protein kinase C contributes to downregulation by bryostatin. Am J Physiol. 1996;271(1 Pt 1):C304–11. [PubMed: 8760059]
39. Grant S. Modulation of ara-C induced apoptosis in leukemia by the PKC activator bryostatin 1. Front Biosci. 1997;2:d242–52. [PubMed: 9195893]
40. Grant S, Jarvis WD, Swerdlow PS, Turner AJ, Traylor RS, Wallace HJ, et al. Potentiation of the activity of 1-beta-D-arabinofuranosylcytosine by the protein kinase C activator bryostatin 1 in HL-60 cells: Association with enhanced fragmentation of mature DNA. Cancer Res. 1992;52(22):6270–8. [PubMed: 1423273]
41. Jarvis WD, Povirk LF, Turner AJ, Traylor RS, Gewirtz DA, Pettit GR, et al. Effects of bryostatin 1 and other pharmacological activators of protein kinase C on 1-[beta-D-arabinofuranosyl]cytosine-induced apoptosis in HL-60 human promyelocytic leukemia cells. Biochem Pharmacol. 1994;47(5):839–52. [PubMed: 8135859]
42. Mihara K, Yoshida T, Ishida S, Takei Y, Kitanaka A, Shimoda K, et al. All-trans retinoic acid and interferon-alpha increase CD38 expression on adult T-cell leukemia cells and sensitize them to T cells bearing anti-CD38 chimeric antigen receptors. Blood Cancer J. 2016;6:e421. [PubMed: 27176797]
43. Weitman S, Langevin AM, Berkow RL, Thomas PJ, Hurwitz CA, Kraft AS, et al. A Phase I trial of bryostatin-1 in children with refractory solid tumors: a Pediatric Oncology Group study. Clin Cancer Res. 1999;5(9):2344–8. [PubMed: 10499603]

Translational Relevance:

CD22 CAR T cells induce remission in approximately 70% of patients with relapse and refractory ALL, including those with CD19 antigen loss after CD19 targeted immunotherapy. However, most will relapse with reduced CD22 antigen density. Here, we describe the implications of low antigen density on the activity of CD22 CAR T cells. Using *in vivo* modeling, we demonstrate reduced activation, expansion, and persistence in CAR T cells when exposed to leukemia with low CD22 expression. Finally, we identify that Bryostatin1, a drug already safely administered to humans, can increase CD22 expression levels, resulting in improved durability of CAR response. Based on these findings, we propose that Bryostatin1 may be combined with CD22 CAR therapy in patients to enhance durability of responses.

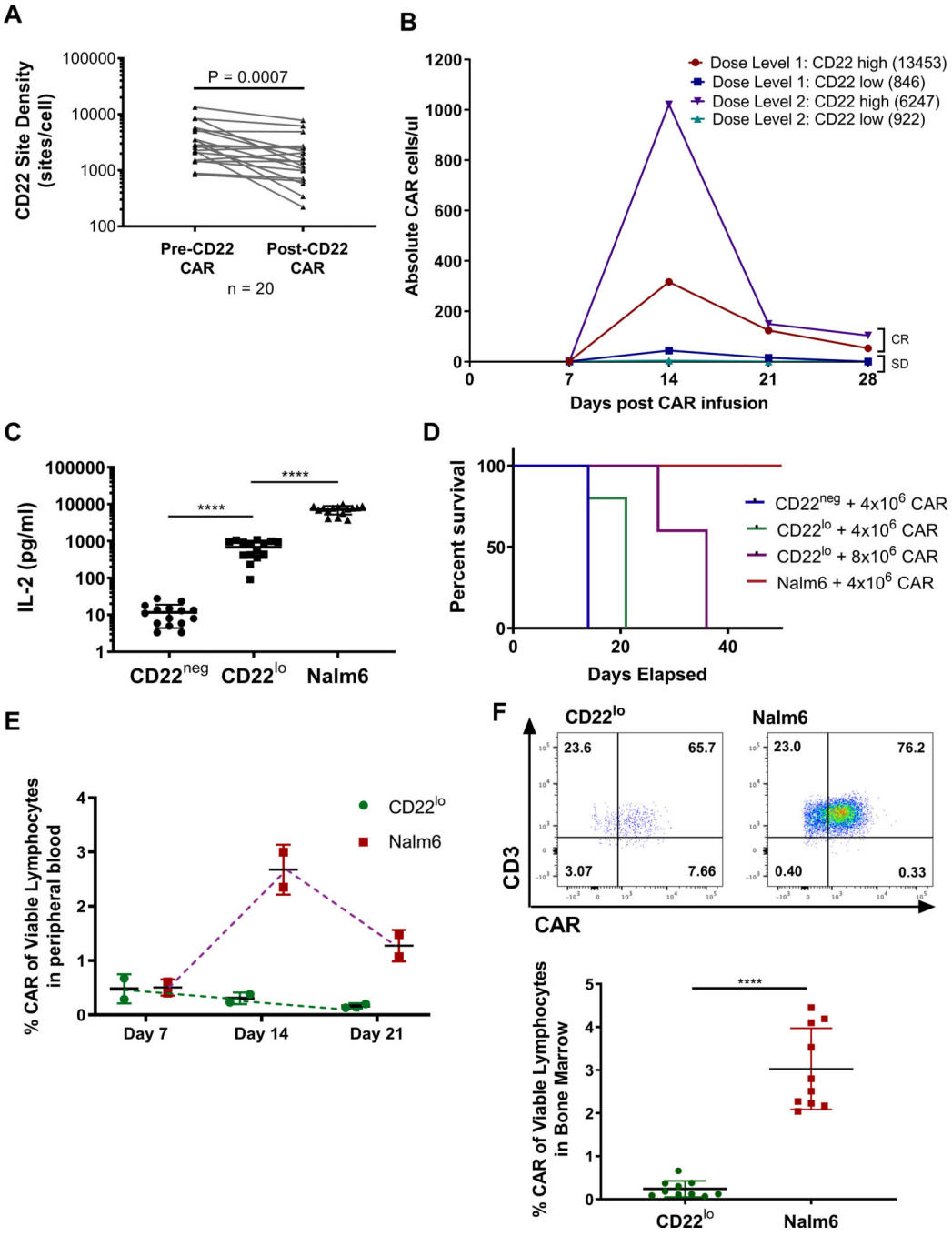

Figure 1: CD22 expression decreases following CD22 CART, and decreased CD22 expression attenuates CART expansion and persistence.

(A) Patient samples pre- and post-CD22 CAR therapy were evaluated for CD22 expression using Quantibrite-PE bead evaluation. Statistics were performed using Wilcox test. (B) Four separate CD22 CART patient samples – two at Dose level 1 and two at Dose level 2 – were evaluated for site density using Quantibrite-PE analysis and CD22 CAR using flow cytometry. (CR – MRD-negative Complete Response; SD – Stable Disease) (C) 1×10^5 tumor cells were co-cultured with 1×10^5 CD22 CAR cells from CD22 CART patient samples for 18hrs. Supernatant was evaluated by Meso Scale Multiplex pro-inflammatory

cytokine panel. Statistics were calculated using unpaired t-test (**** $p<0.0001$, *** $p<0.0002$, ** $p<0.0021$). (D) Kaplan-Meier curves comparing $CD22^{neg}$ to $CD22^{lo}$ and Nalm6 leukemia-bearing mice with different CART doses. (E) Peripheral blood was collected from mice at interval timepoints and assessed for CAR expansion using flow cytometry and analyzed on Fortessa flow machine. (F) CAR expansion was evaluated from bone marrow of mice 16 days after tumor injection. Cells were stained for flow cytometry and analyzed on Fortessa flow machine. Statistics were calculated using Mann-Whitney test (**** $p < 0.0001$, * $p < 0.0332$).

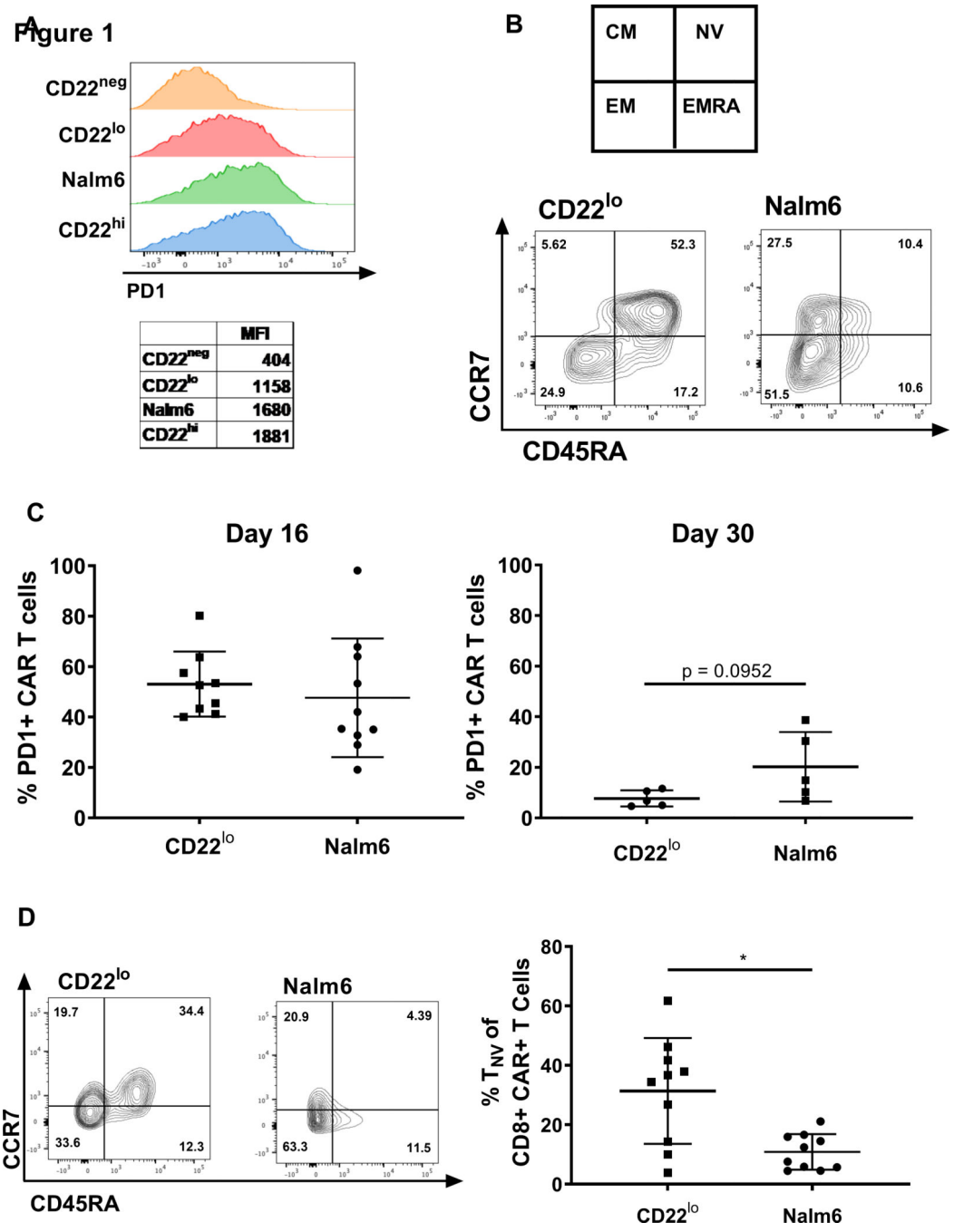

Figure 2: Site density affects early activation and memory phenotype of CD22 CART cells.

(A) Site density cell lines were co-incubated with CD22 CART for 24 hours, and PD1 expression was stained flow cytometry and analyzed on Fortessa flow machine. (B) CD22 CAR was co-cultured *in vitro* with $CD22^{lo}$ or Nalm6 leukemia for 8 days and cells were evaluated using flow cytometry and analyzed on Fortessa flow machine. (C) Cells were extracted from CD22 CAR treated $CD22^{lo}$ or Nalm6 NSG mice 16 or 30 days after tumor injection. Cells were stained for flow cytometry and analyzed on Fortessa flow machine. (D) Cells were extracted from CD22 CAR treated $CD22^{lo}$ or Nalm6 NSG mice 16 days

following tumor injection. Cells were stained for flow cytometry and analyzed on Fortessa flow machine. This data was reproducible across two separate experiments. Statistics were calculated using Mann-Whitney test (**** $p < 0.0001$, * $p < 0.0332$).

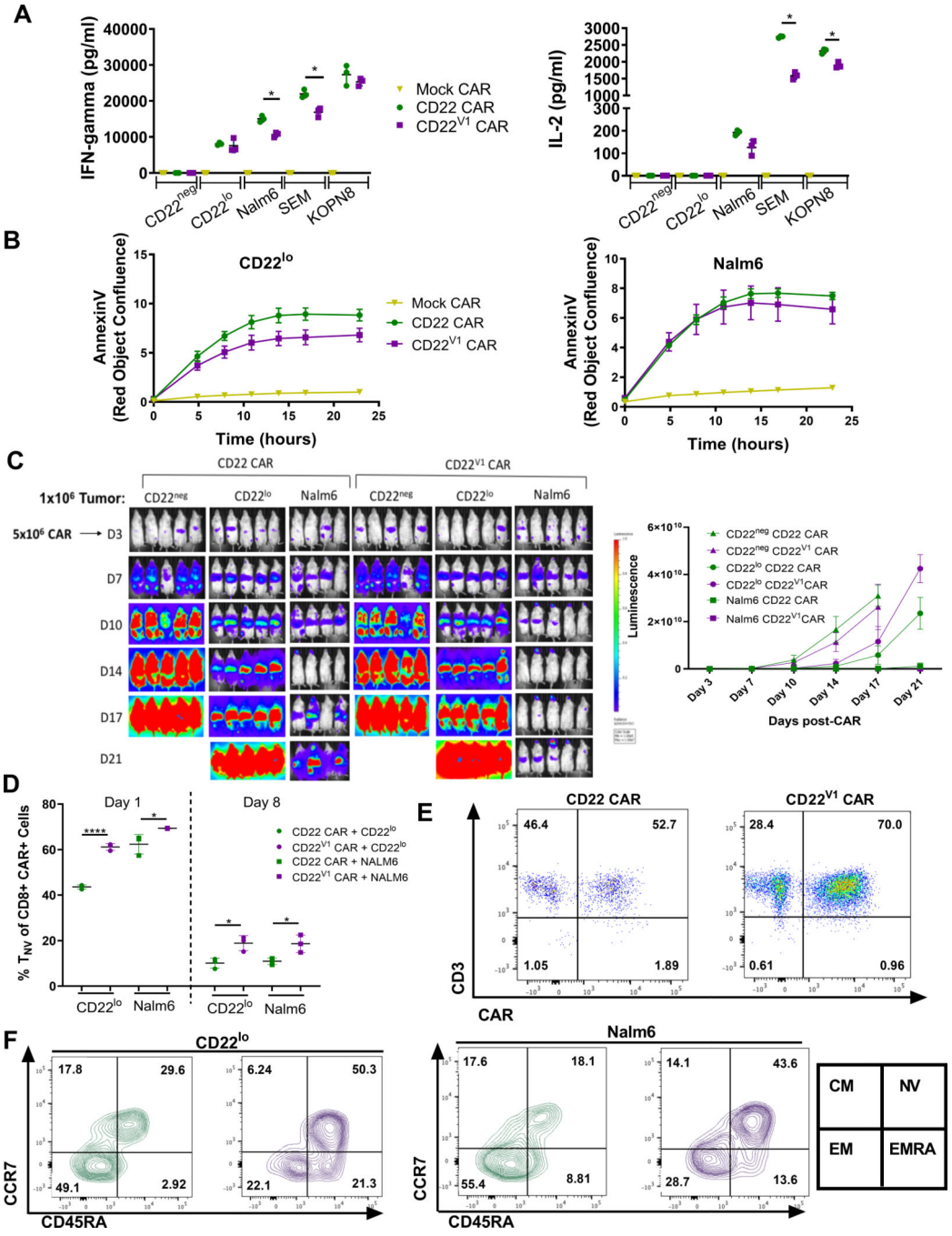

Figure 3:

(A-B) 1×10^5 tumor cells were co-cultured with 1×10^5 Mock, CD22, or $CD22^{V1}$ CAR and assessed for (A) IFN-γ and IL-2 cytokines by ELISA from cell culture supernatants (statistics were calculated using paired t test (* $p<0.0332$)) or (B) AnnexinV staining was assessed over time using IncuCyte ZOOM. This data is representative of two separate experiments and was consistent across 2 different E:T ratios. (C) NSG mice were injected with 1×10^6 GPF-positive $CD22^{neg}$, $CD22^{lo}$, or Nalm6 tumor cells on Day 0. On Day 3, 5×10^6 CD22 or $CD22^{V1}$ CAR were injected for treatment. Mice were imaged using IVIS

technology and luciferin-D IP injections. Luminescence quantification is shown on the right. This data is representative of two separate experiments. (D) CD22 or $CD22^{V1}$ CART were co-incubated with tumor cells. On Days 1 and 8, CAR was harvested, stained for flow cytometry, and analyzed on Fortessa Flow machine. Statistics were calculated using unpaired t-test (* $p < 0.0332$). (E-F) Mice were injected with $CD22^{lo}$ or Nalm6 leukemia on Day 0. 5×10^6 CD22 CAR T cells were administered on Day 3 and mice were sacrificed on Day 16. Bone marrow cells were stained for flow cytometry and analyzed on Fortessa Flow machine. Statistics were calculated using unpaired t-test (**** $p<0.0001$, * $p<0.0332$).

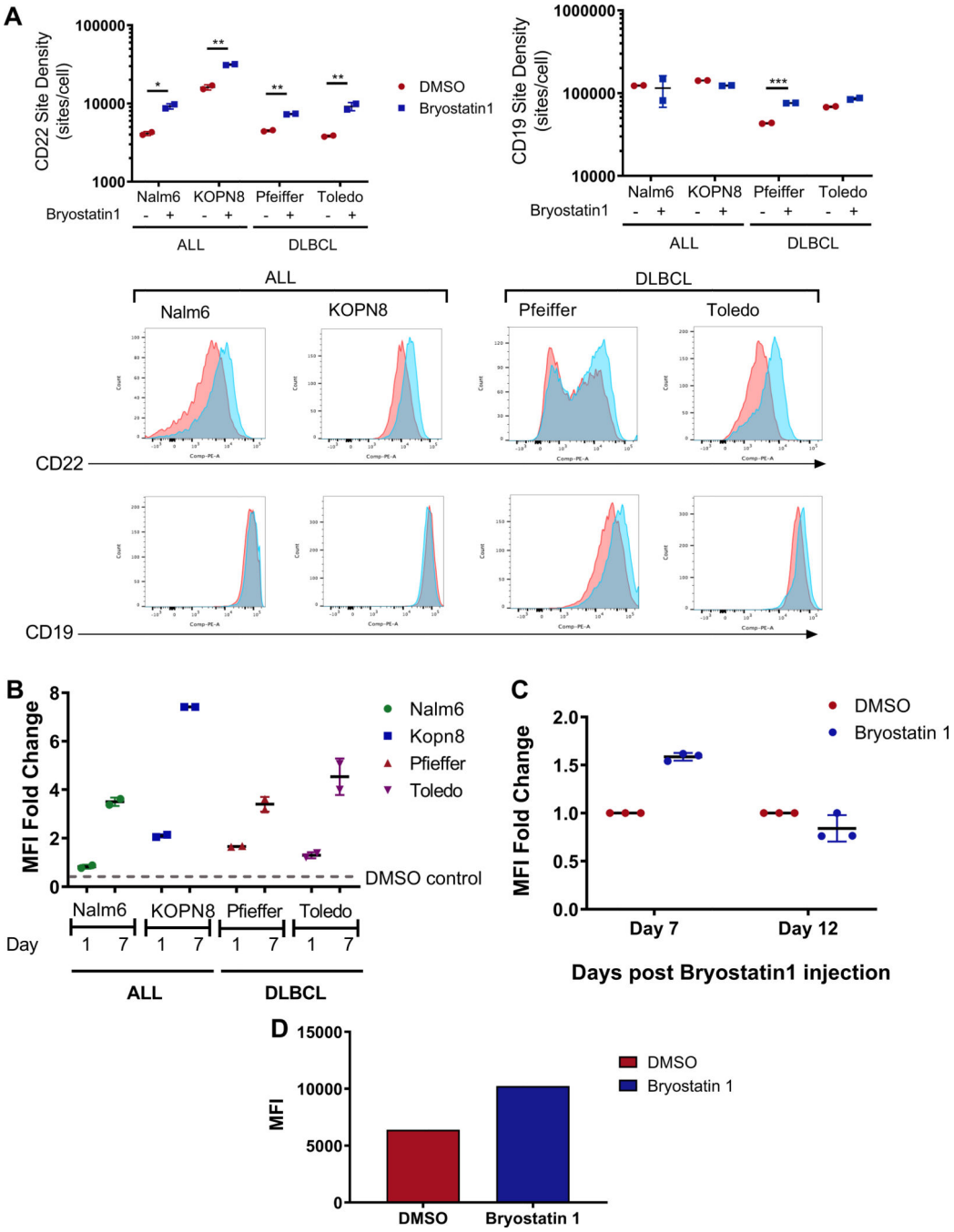

Figure 4: Bryostatin1 upregulates CD22, but not CD19, and CD22 increased expression is durable for 1 week after drug exposure.

(A) Four cell lines were co-incubated with 1nM Bryostatin1 for 24 hours and analyzed using flow cytometry one day after Bryostatin1 exposure. Site density was analyzed through use of standardized Quantibrite-PE beads. Statistics were calculated using unpaired t-test (*** <0.0002, ** p<0.0021, * p<0.0332). (B) Cell lines were co-incubated with 1nM Bryostatin1 for 24 hours, washed, and analyzed using flow cytometry at 1 and 7 days after Bryostatin1 exposure. MFI fold change = CD22 $MFI^{Bryostatin1}$/CD22 MFI^{DMSO}. (C) NSG mice were injected with 1×10^6 GPF-positive Nalm6 leukemia cells on Day 0. Bryostatin1 was

administered at 0.8ug/kg on Day 3. Mice were sacrificed 7 and 12 days after Bryostatin1 injection and CD22 was evaluated through flow cytometry. MFI fold change = CD22 $MFI^{Bryostatin1}$/CD22 MFI^{DMSO}. (D) CD22-low relapse patient-derived xenograft cell line was cultured *in vitro* with 1nM Bryostatin1 for 24 hours and measured for CD22 expression using CD22 antibody.

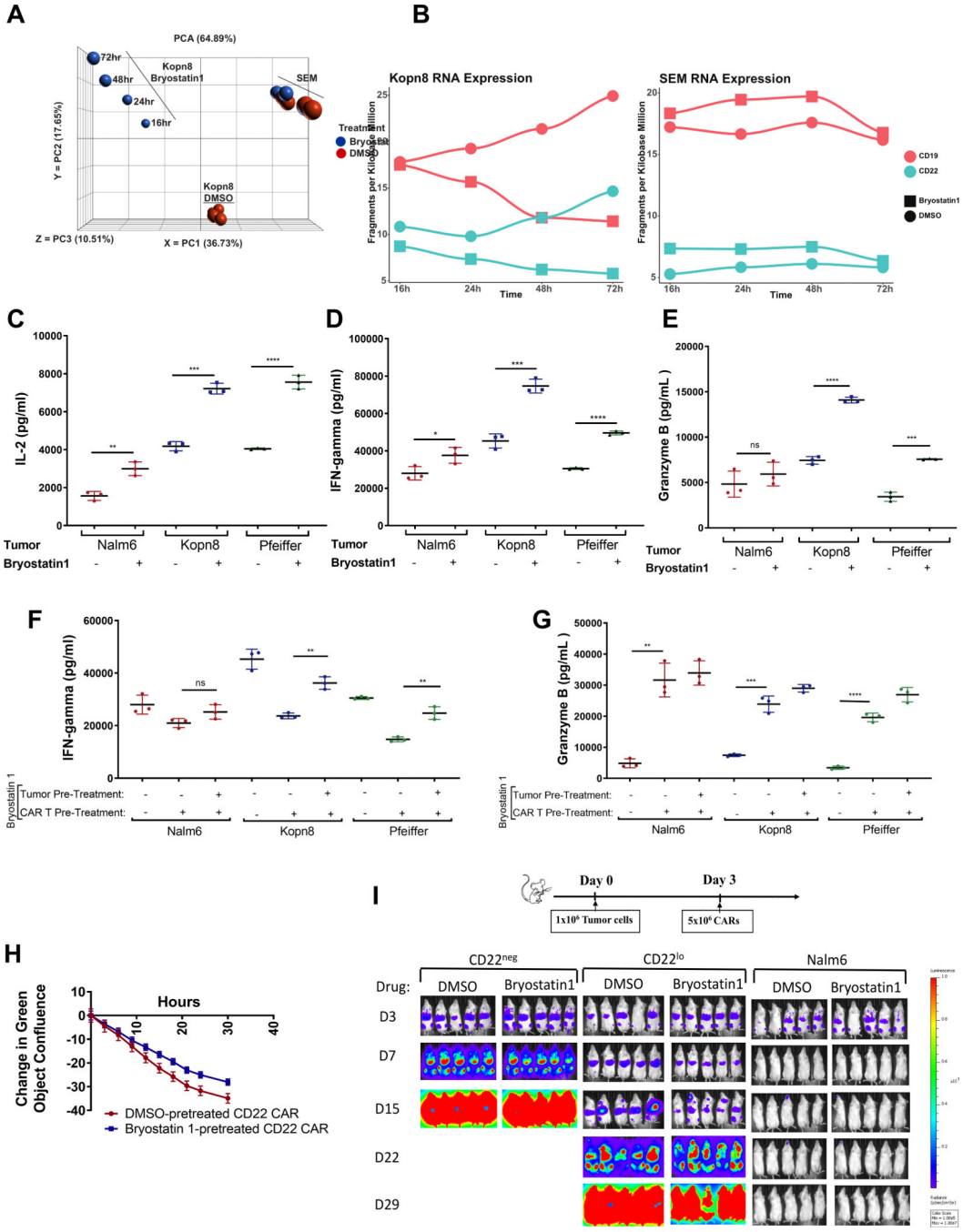

Figure 5: RNAseq analysis shows no substantive difference in CD22 expression; Bryostatin1-mediated increased CD22 augments CART potency; and CART exposure to Bryostatin1 decreases IFN-gamma production, but increases Granzyme B production, and does not adversely affect tumor clearance *in vitro* or *in vivo*.

(A-B) KOPN8 or SEM cell lines were exposed to 1nM Bryostatin1 for 16, 24, 48, or 72 hours. RNA was extracted and analyzed by RNAseq. (C-E) Cell lines were co-incubated with 1nM of Bryostatin1 for 24 hours. Then 1×10^5 target tumor cells were co-cultured with 1×10^5 CD22 CAR for 16hrs. IL-2 (C), IFN-γ (D), and granzyme B (E) were measured by ELISA from cell culture supernatants. Statistics were calculated using unpaired t-test (****

p<0.0001, *** p<0.0002, ** p<0.0021, * p<0.0332). (F-G) CD22 CART cells were co-incubated with 1nM of Bryostatin1 for 24 hours and washed. Then 1×10^5 target tumor cells were co-cultured with 1×10^5 CD22 CAR for 18 hrs. IFN-γ (F), and granzyme B (G) were measured by ELISA from cell culture supernatants. Statistics were calculated using unpaired t-test (**** p<0.0001, *** p<0.0002, ** p<0.0021). (H) Mock or CD22 CAR T cells were co-incubated at 1:1 effector-to-target ratio with either $CD22^{neg}$, $CD22^{lo}$ or Nalm6 cells. Cell death was monitored by loss of GFP-positive cells using IncuCyte ZOOM. (I) NSG mice were injected with $CD22^{neg}$, $CD22^{lo}$, or Nalm6 on Day 0, CD22 CAR T cells on Day 3, and then were given either DMSO control or Bryostatin1 at 40ug/kg once weekly for 2 weeks. Leukemia progression was monitored using IVIS technology and luciferin-D IP injections.

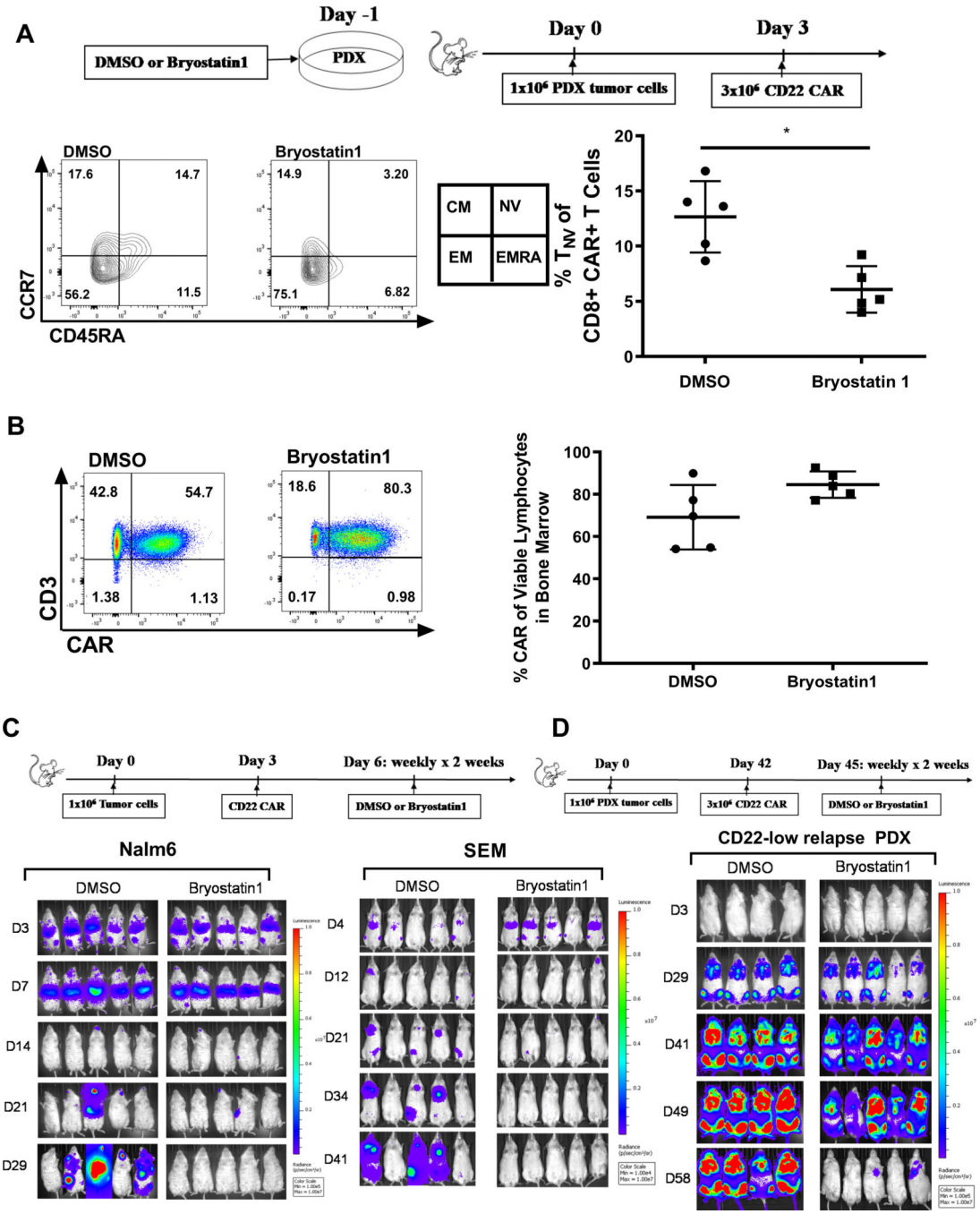

Figure 6: Bryostatin1 treatment pre-CAR infusion alters T cell phenotype without T cell exhaustion, and post-CAR infusion improves durability of remission *in vivo*.

(A) Nalm6 cells were exposed to 1nM Bryostatin1 for 24 hours, then injected into mice on Day 0. CD22 CAR T cells were administered on Day 3 and mice were sacrificed on Day 10. Bone marrow cells were stained for flow cytometry and analyzed on Fortessa Flow machine. Statistics were calculated using unpaired t-test (* $p < 0.0332$). (B) NSG mice were injected with Nalm6 on Day 0, CD22 CART on Day 3, and then were given either DMSO control or Bryostatin1 at 40ug/kg once weekly for 2 weeks. Mice were sacrificed 30 days after tumor injection. Cells were stained for flow cytometry and analyzed on Fortessa Flow machine. (C)

NSG mice were injected with 1×10^6 GPF-positive Nalm6 or SEM tumor cells on Day 0. On Day 3, either 3×10^6 (Nalm6) or 2×10^6 (SEM) Mock or CD22 CAR were injected for treatment. Mice were given 40ug/kg of Bryostatin1 or DMSO once weekly for 2 weeks. Mice were imaged using IVIS technology and luciferin-D IP injections. (D) NSG mice were injected with 1×10^6 GPF-positive PDX tumor cells on Day 0. On Day 42, 3×10^6 Mock or CD22 CAR were injected for treatment. Mice were given 40ug/kg of Bryostatin1 or DMSO once weekly for 2 weeks starting on Day 45. Mice were imaged using IVIS technology and luciferin-D IP injections.